

pH-responsive size-shrinkable mesoporous silica-based nanocarrier for improved tumor penetration and therapeutic efficacy

Yongju He^{a,*}, Xingyu Fan^a, XIAOZAN Wu^b, Taishun Hu^a, Fangfang Zhou^c, Songwen Tan^d, Botao Chen^{c,*}, Anqiang Pan^a, Shuquan Liang^a and Hui Xu^f

^a School of Material Science and Engineering, Central South University, Changsha, Hunan 410083, China

^b Science Park, Central South University, Changsha, Hunan 410083, China

^c Department of Neurology, the Second Xiangya Hospital, Central South University, Changsha, Hunan 410011, China

^d Xiangya School of Pharmaceutical Sciences, Central South University, Changsha, Hunan 410013, China

^e Department of Hepatobiliary Surgery, Hunan Provincial People's Hospital The First-Affiliated Hospital of Hunan Normal University, Changsha, Hunan, China

^f Institute of Super-Microstructure and Ultrafast Process in Advanced Materials, School of Physics and Electronics, Central South University, Changsha, Hunan 410083, China

Corresponding author: heyongju@csu.edu.cn & hnsrmmy_cbt@126.com

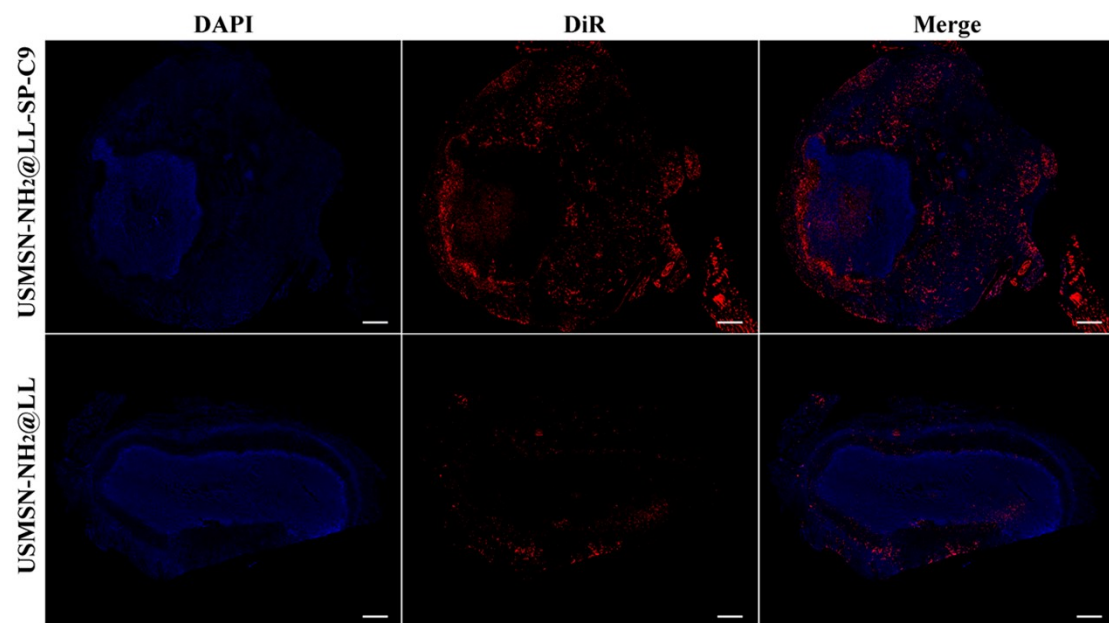


Figure S1. Whole slice scanning to examine the in vivo tumor penetration of USMSN-NH₂@LL-SP-C9 and USMSN-NH₂@LL. Bar scale 500 μ m.

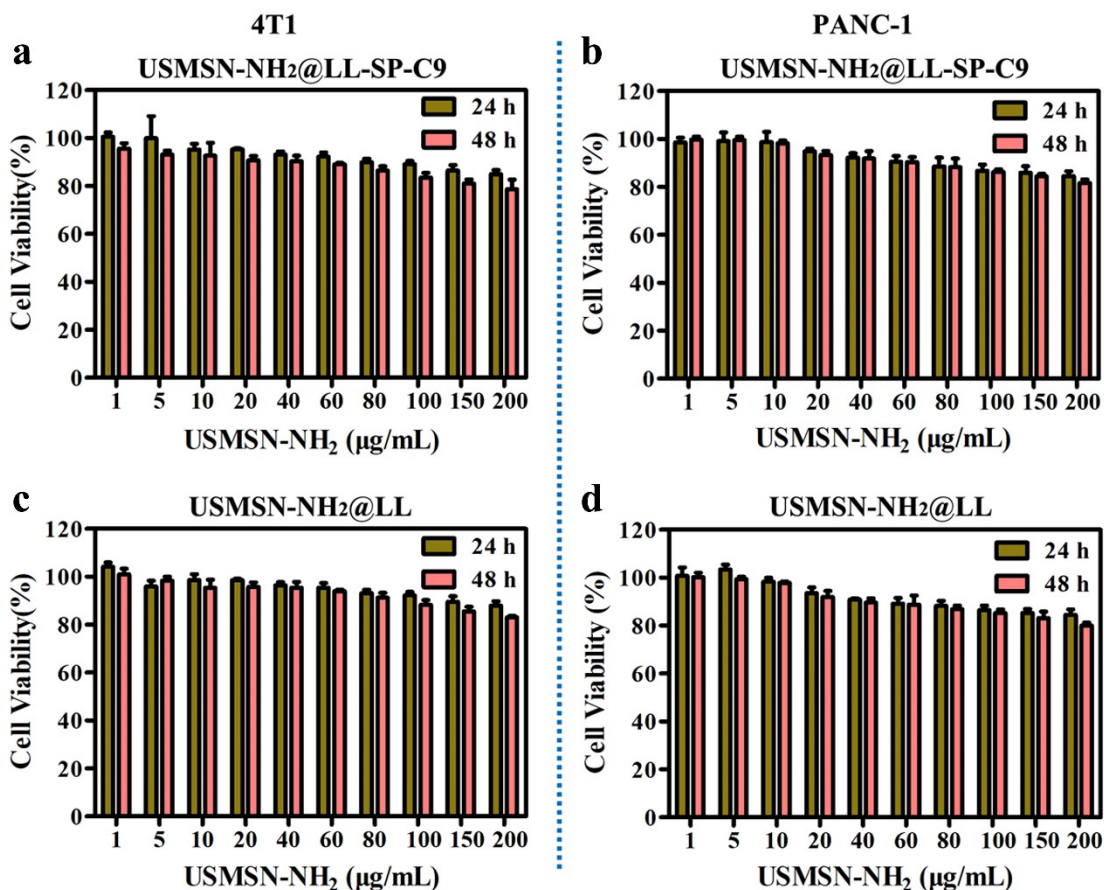


Figure S2. The cytotoxicity of blank USMSN-NH₂@LL-SP-C9 and blank USMSN-NH₂@LL against (a, c) 4T1 and (b, d) PANC-1 cells.

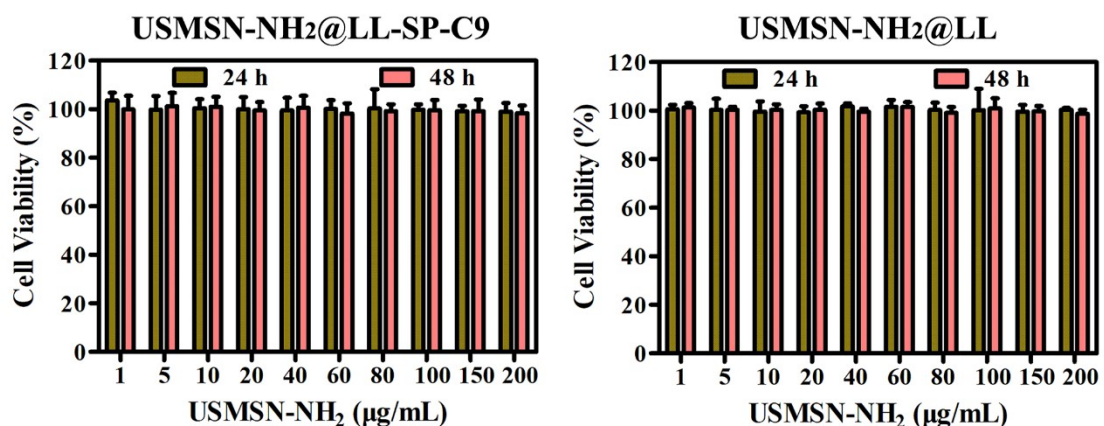


Figure S3. The cytotoxicity of blank USMSN-NH₂@LL-SP-C9 and blank USMSN-NH₂@LL against normal MOVAS cells.

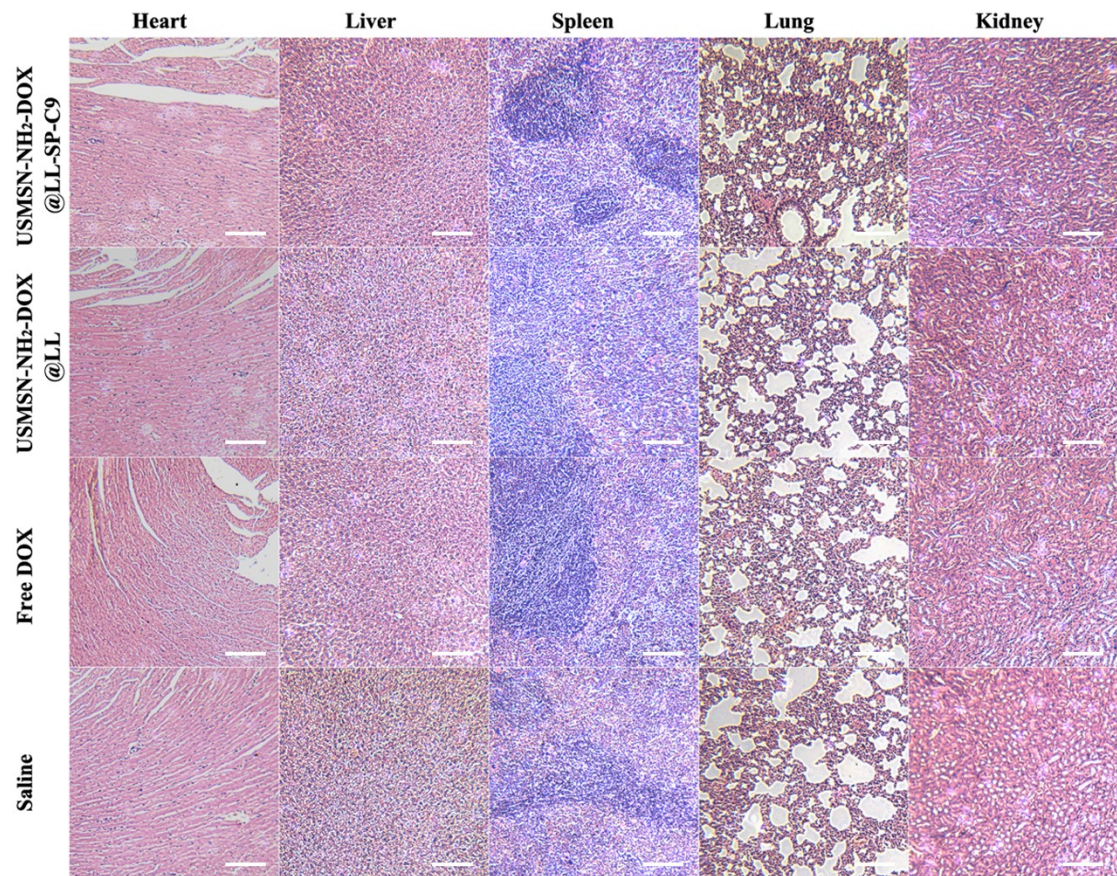


Figure S4. H&E images of the major organs taken from mice-bearing 4T1 tumor on the day 10 post treatment. Bar scale 100 μ m.

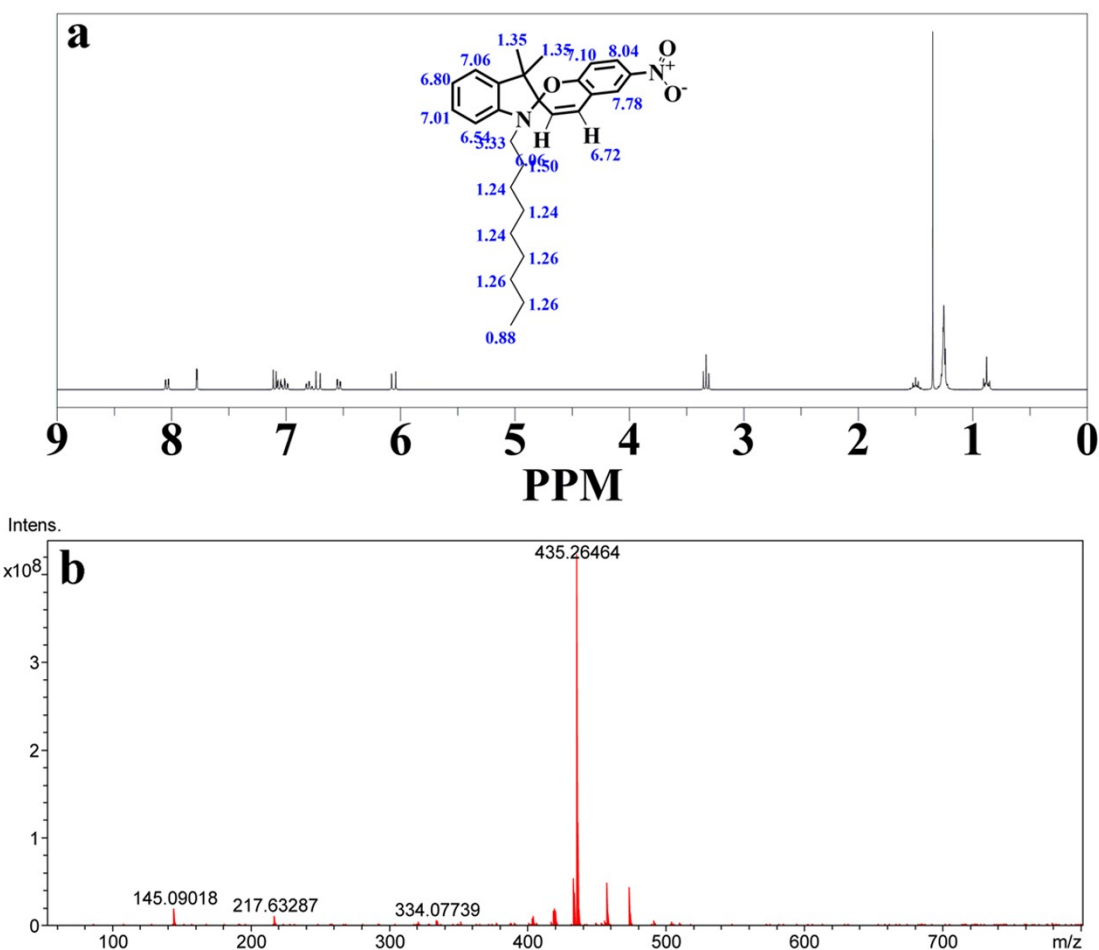


Figure S5. (a) ^1H NMR spectrum and estimation (inset) of SP-C9, and (b) high mass spectrum of SP-C9.

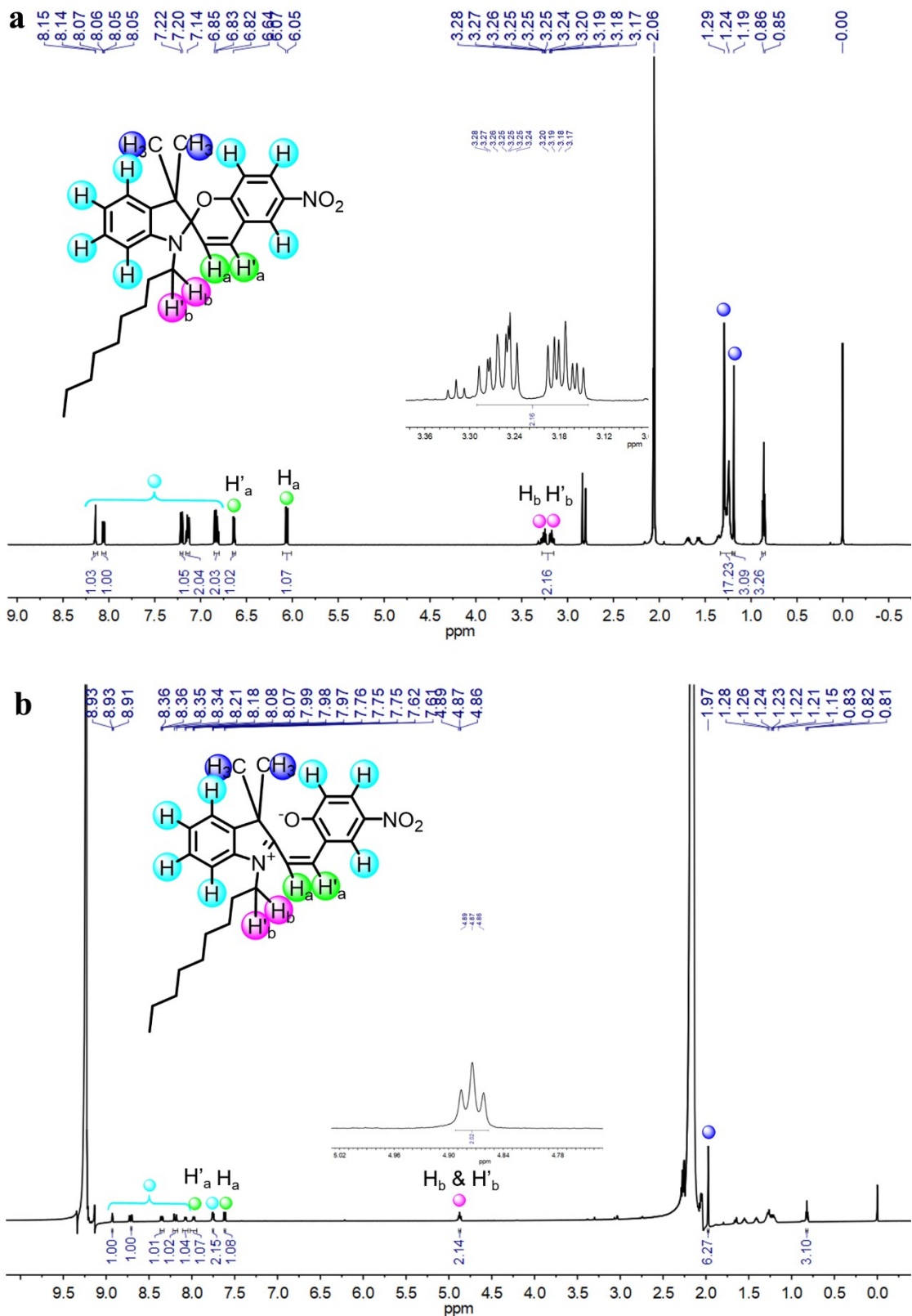


Figure S6. ^1H NMR spectrum of SP-C9 in acetone-d6 with neutral (a) and acidic pH (b).